Determination of Stress Concentration for Orthotropic and Isotropic Materials Using Digital Image Correlation (DIC)

Mhalla Mohamed Makki and Bouraoui Chokri

Laboratory of Mechanical Engineering, University of Monastir Tunisia
mhallamaki@yahoo.fr,
chokri.bouraoui@enim.rnu.tn

Abstract. The objective of this study was to perform a tensile test on isotropic and orthotropic plates with holes and measured deformations around their hole by using the method of digital image correlation (DIC). The results of this measure were used to determine the local stress at the edge of the hole and measured the net and global stress concentration factor for isotropic and orthotropic materials and see the difference between the two types of materials.

This paper presents an analysis of the net and global stress concentration factor for different hole diameters and their influence on the isotropic and orthotropic material using a camera DIC.

Keywords: orthotropic, isotropic, plate with hole, stress concentration factor, digital image correlation DIC.

1 Introduction

The stress concentration is a local phenomenon that increases the stresses in an area having a geometrical modification of the part. This discontinuity appears in a part of the structure or with the presence of a cut (hole, notch ...). The stress concentration area is often the site of initiation failure, but may also be the cause of a sharp break in the case of a brittle material. Heywood [1] Peterson [2] and Pilkey [3] studied several forms of stress concentration for isotropic materials with a wide range of holes. Howland [4] determined the solution of the rectangular isotropic plate problem with a hole in the center with a tensile load. Peterson and Heywood introduced different equations for a finite plate with different aperture shapes. Lekhnitskii [5] and Tan [6] introduced different formulations for the stress concentration in orthotropic materials. Lekhnitskii derived an equation for an infinite plate with circular holes. And for a finite orthotropic plate Tan has a various equations.

M. Haddar et al. (eds.), *Multiphysics Modelling and Simulation for Systems Design and Monitoring*, Applied Condition Monitoring 2, DOI: 10.1007/978-3-319-14532-7_53

2 Digital Image Correlation (DIC)

The camera allows the use of in situ recording of a burst frame. These are used to measure the displacement fields and local deformation. The principle of image correlation is to compare local travel in the plane perpendicular to the camera between two different images. Comparing a said deformed image and the reference image allows the measure of local movements (Figure 1). The calculations do not take into account the movement of solid body. From these measurements, the local deformations are deducted in the directions of the study design. To determine the displacement at point of the specimen, it is divided into small images and is squared. The grid represents the space between two thumbnail images, they may intersect. The user can therefore play on two adjustable parameters are the size of the thumbnail images and size of the grid. Although it appears to have the perfect pattern thinnest and finest grid in order to gain accurate measurements, this configuration is not always the most suitable. When the grid is too fine, the correlation has a noise significant measurement.

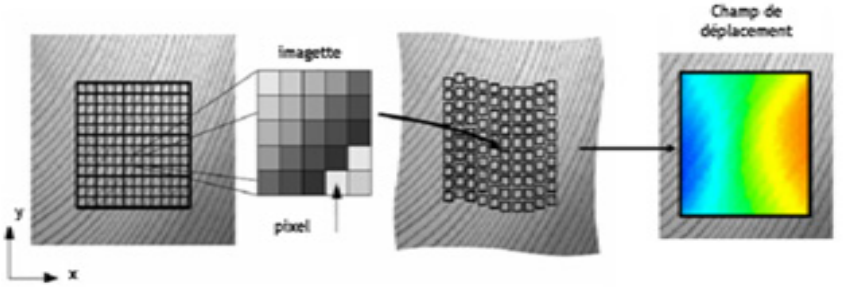

Fig. 1 Principle of image correlation: determining an optimal field of displacement by image analysis. Reference image and images solicited are devisees of series thumbnail images (set of pixels) [7]

This method is implemented on plate specimens with hole than is covered with a white paint before the test. Is then carried out by spraying an artificial marking paint with a speckle pattern on the surface of the material, via a black spray. Thereafter, the image correlation is performed using the standard software ICASOFT® [Icasoft] developed by Fabrice Morestin (Mguil-Touchal and al.1996) [7] to LaMCoS laboratory of INSA Lyon (Example Icasoft image with Figure 2). The principle is used to match two (original and distorted) images by comparison pixel by pixel with using a criterion based on the grid level in order to evaluate the displacement field and the corresponding strain.

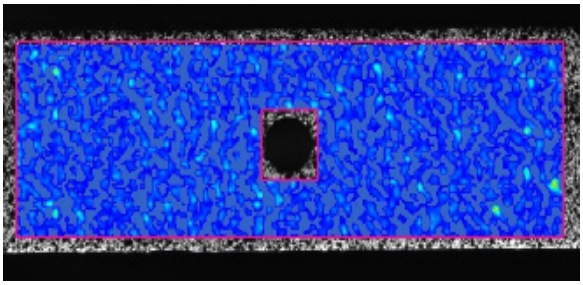

Fig. 2 Example of an image with camera DIC

3 Experimental Study

The equipment used for the tests of uniaxial tension is: traction machine EZ20 with computer controlled device and image acquisition, including a lamp for lighting. The tests summers Films has captured with the camera positioned facing the test, all using software (Icasoft, INSA Lyon, LAMCOS-MSE) to determine displacement fields and strain. See Figure 3:

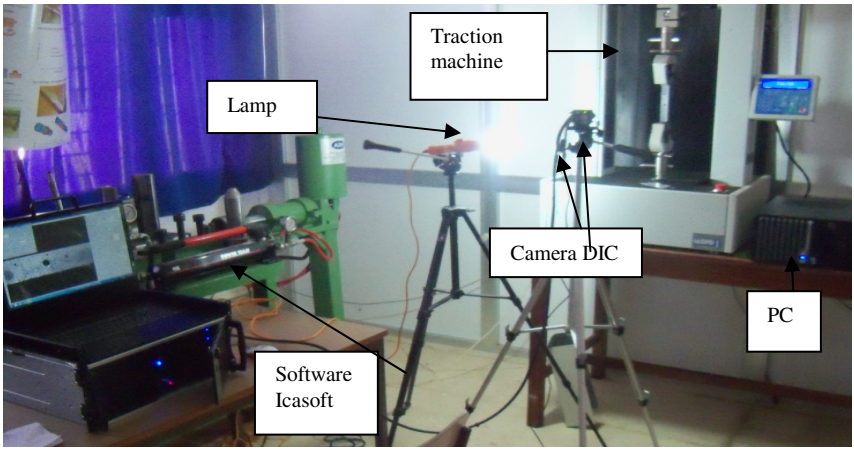

Fig. 3 Diagram of the mechanical acquisition data and digital images with a uniaxial tensile test.

Tensile tests were carried out in a universal testing range of the EASY TEST Machine combine flexibility with exceptional usability, EZ20 model with transverse hydraulically setting with constant velocity about 2 mm / min, with ambient temperature.

Tensile tests were performed according to standard ASTM D3039 [8] (Figure 4), using a minimum of twelve specimens (The most current specimens to ASTM D3039 has a constant rectangular cross-sectional dimensions: 250 mm long x 25 mm wide x 2 mm thick test .A typical speed for standard test samples of 2 mm / min) for each family of laminate.

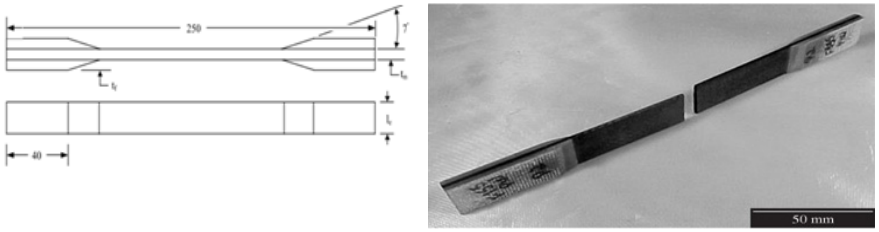

Fig. 4 Standard ASTM D3039 [20]

The specimens were made from carbon / epoxy with 0.22 mm thick. The tapes were strength carbon fibers (T700) high strength unidirectional of M21 Hexcel epoxy resin (35% resin). The plate contains eight unidirectional layers [0/90] 2s laminate with a total thickness of 1.76 mm. These tacking sequences have helped to get an overview of the evaluation with different types of damage in notched specimens under uniaxial loading using DIC.

The specimens were prepared by bonding the end of glass fiber / epoxy laminate legs. This procedure resulted in the available 150 mm2 of the sample for the tensile test surface. Figure below shows the laminated specimens with different diameters:

Fig. 5 specimens of plate

4 Results

With an ambient temperature, it was two families of tests: steel and composite plates with different hole in the center with the same size and speed of loading (Figure 6) .on notice the break in the steel is still in hole and perpendicular to the loading, against composite the breakage is around the hole but the orientation of crack always followed the direction of tissue .In our example we have a orientation tissue [0.90]2s. So the crack almost perpendicular to the load.

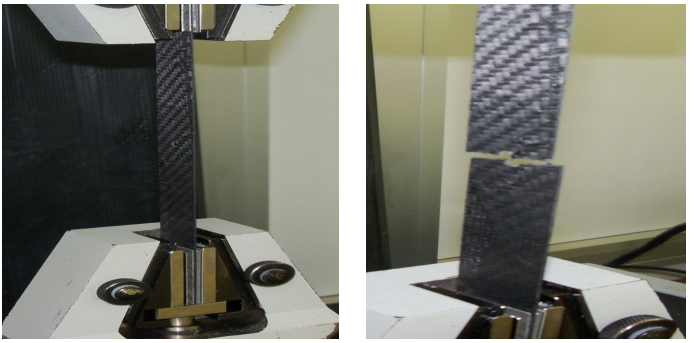

Fig. 6 Tensile test for a composite plate with hole (a=4mm)

Thereafter we can plot the stress-time curve for the composite plate (Figure7) such that we can see the first damage and then the fiber break with the total damage:

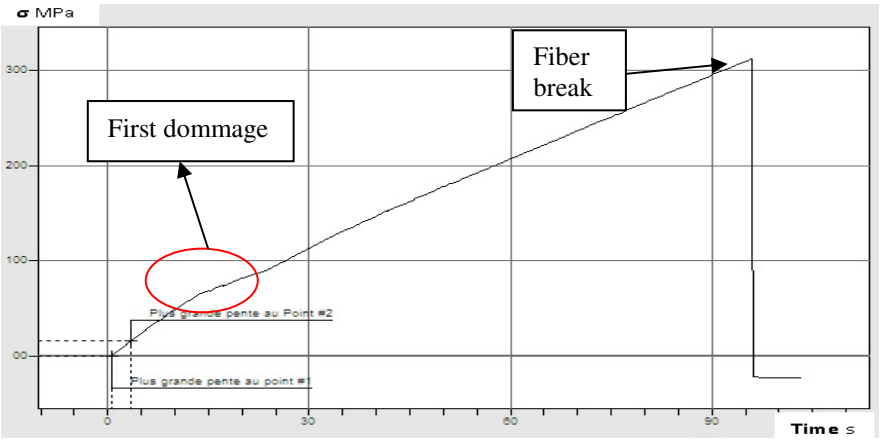

Fig. 7 Stress-Time curve for a composite plate with hole (a=4mm)

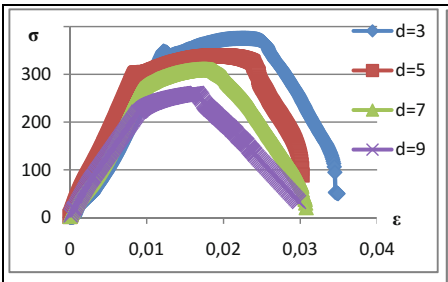

Fig. 8 Stress-Strain curve for a steel plate with different diameters

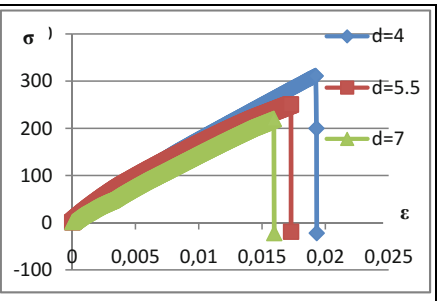

Fig. 9 Stress-Strain curve for a composite plate with different diameters

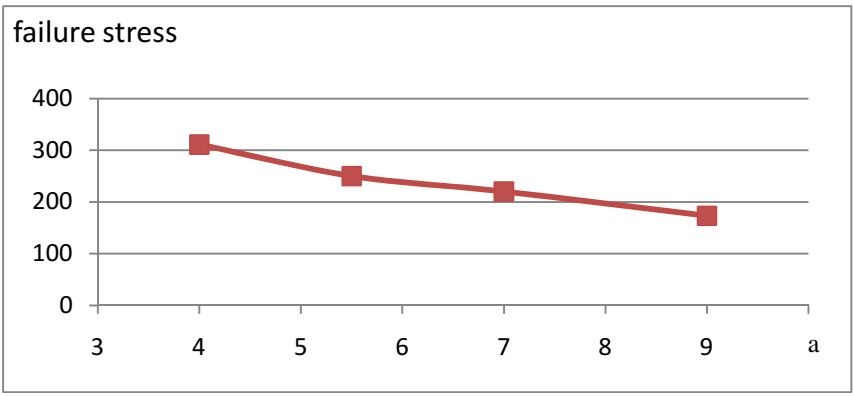

Fig. 10 Variation of failure stress with a different hole diameter

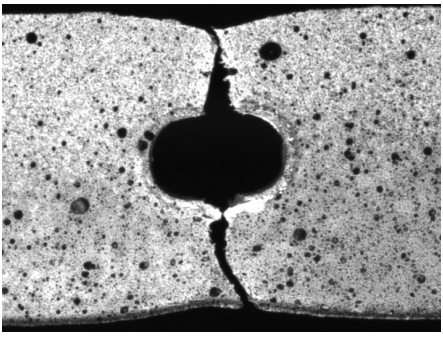

Fig. 11 Image of damaged Steel plate

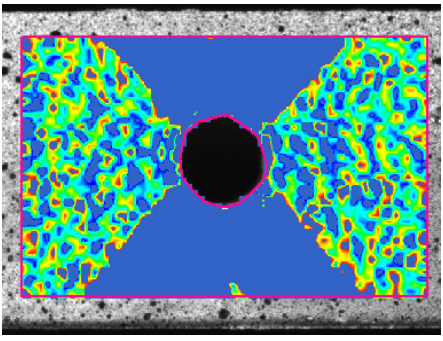

Fig. 12 Image of damaged steel plate with camera DIC

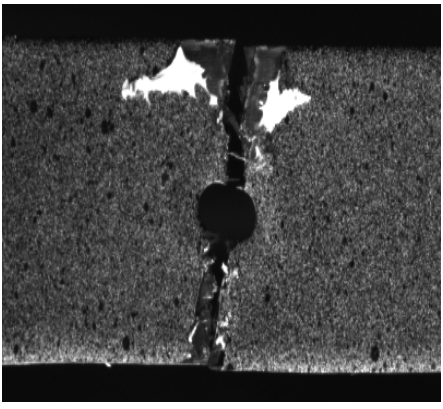

Fig. 13 Image of damaged composite plate

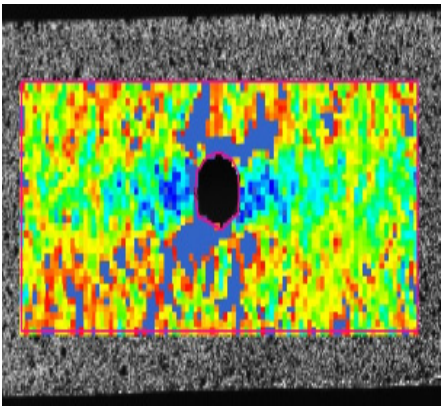

Fig. 14 Image of damaged composite plate with camera DIC

Before beginning the analysis of the diameters influence on the intensity of stress concentration, it is necessary to present the general appearance of the stress respect to strain (Figures 8-9).

In addition, it is important to know the failure stress of each hole diameter to estimate its influence on the resistance plate (Figure 10).

Note that the failure stress down with increasing of notch diameter .We conclude that the hole size has a very important role in the resistance of plaque rupture. For this we used the method of image correlation with DIC camera that gives travel and local deformations to determine the local stresses at geometric discontinuity. Thereafter we can see in Figures (11-18) images of holes in steel and composite plates given by DIC camera:

Figure (15) shows the variation of the longitudinal strain (ε11) along the y axis and passing through the center hole, this variation measured from DIC camera.

In These planar structures, the state of stress is fairly well represented by a plane stress tensor, that:

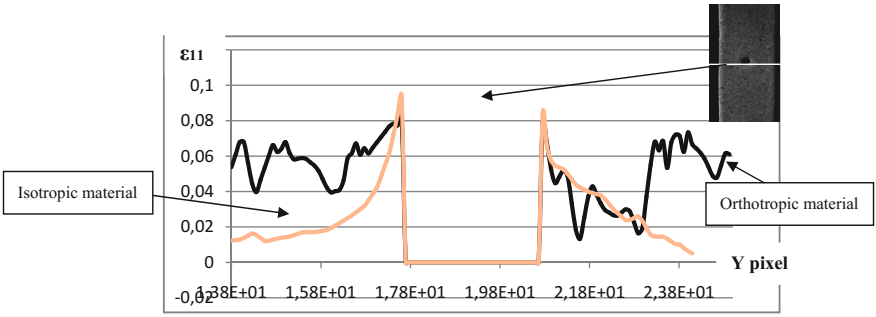

Fig. 15 Variation of the longitudinal strain (ε11) along the y axis

$$\begin{Bmatrix} \sigma_{11} \\ \sigma_{22} \\ \sigma_{12} \end{Bmatrix} = \begin{Bmatrix} Q_{11} & Q_{12} & 0 \\ Q_{12} & Q_{22} & 0 \\ 0 & 0 & Q_{66} \end{Bmatrix} \begin{Bmatrix} \epsilon_{11} \\ \epsilon_{22} \\ 2\epsilon_{12} \end{Bmatrix}$$

Subsequently, the longitudinal stress around the hole can be calculated from the deformation field (ε11 and ε22) obtained from DIC:

$$\sigma_{11} = \frac{E_{11}\varepsilon_{11}}{[1 - \nu_{12}^2(E_{22}/E_{11})]} + \frac{\nu_{12}E_{22}\varepsilon_{22}}{[1 - \nu_{12}^2(E_{22}/E_{11})]}$$

Finally we can plot the stress concentration ($Kt = \sigma_{max} / \sigma_{nom}$ avec $\sigma_{max} = \sigma_{11}$) with a different hole diameters for steel and composite (carbon / epoxy) materials.

5 Theoretical Coefficient of Global Stress Concentration

Theoretical coefficient of stress concentration is defined as the ratio of the actual maximum stress in the zone of discontinuity (notch, hole, for example) to the nominal stress in the section:

$$Kt = \sigma_{max} / \sigma_{nom}$$

σ_{max} : Is calculable by numerical methods such as finite element method or by analytical methods for simple geometries. It is also measured by the technical analysis of experimental constraints such as photo-elasticity or DIC methods.

σ_{nom} : Is calculable using the formulas of strength materials, considering the specimen like a bar or plate without account the geometric discontinuity.

$$\sigma_{nom} = \frac{F}{2wh}$$

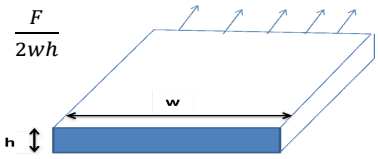

With F: traction, uniform on edges of plate.
w: width of the plate.
h : plate thickness.

6 Evolution of the Global Stress Concentration with Hole Diameter

6.1 Case of Isotropic Material

For a rectangular plate with a circular hole in the middle and subjected to a tensile loading in one direction. It occurs around the hole increasing the value of the stress that is characterized by the stress concentration factor Ktg Howland [9]:

$$k_{tg} = 0.284 + \frac{2}{\left(1 - \frac{2r}{w}\right)} - 0.6\left(1 - \frac{2r}{w}\right) + 1.32\left(1 - \frac{2r}{w}\right)^2$$

6.2 Case of Orthotropic Material (Composite)

For a thin composite plate (assumed orthotropic) infinite (w >> r) with a central hole. The coefficient Kt is obtained by Lekhnitskii [5]:

$$K_t = 1 + \sqrt{2\left(\left(\sqrt{E_x/E_y} - v_{xy}\right) + E_y/G_{xy}\right)}$$

In our case, the study focuses on an infinite orthotropic plate 3D is made of carbon /epoxy (HR [0/90] 2s) .According of Table 1 Kt equal to 5.24 for an infinite orthotropic plate.

According to the investigation of Heywood [1] on a rectangular orthotropic plate with center hole under the action of unidirectional axial load, the factor is introduced in the form of the following equation:

$$\frac{K_{Tg}^{\infty}}{K_{Tg}} = \frac{3\left(1-\frac{a}{W}\right)}{2+\left(1-\frac{a}{W}\right)^{3}} + \frac{1}{2}\left(\frac{a}{W}M\right)^{6}\left(K_{T}^{\infty} - 3\left(1-\left(\frac{a}{W}M\right)^{2}\right)\right)$$

With

$$M^{2} = \frac{\sqrt{1-8\left[\frac{3\left(1-\frac{a}{W}\right)}{2+\left(1-\frac{a}{w}\right)^{3}} - 1\right]} - 1}{2\left(\frac{a}{W}\right)^{2}}$$

7 The Theoretical Value of the Net Stress Concentration

Another way to determine the stress concentration is the application of the average normal stress across the net section instead of the hole width of the plate (global surface).

$$\sigma_{nom} = \frac{F}{2(w-a)h}$$

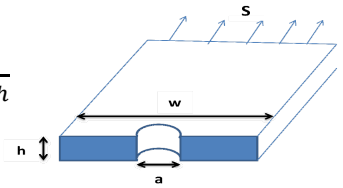

This concentration is known as the net concentration of stresses K_{Tn} [9, 1] and can be related to the global stress concentration factor K_{Tg} by:

$$K_{Tn} = K_{Tg}(1\text{-}a/w)$$

8 Validation by Comparison with the Results of the FE Analysis

8.1 Modelisation with Finite Elements

To validate our work can be compared with the results found by finite elements analysis and with literature.
A simulation under "ABAQUS 6.12" software was performed with a mesh-like continuum Shell hexagonal, progressive and refined around the hole. Two systems of different materials are considered:

Table 1 Material Properties orthotropic carbon / epoxy (T700 / M21 [0 90] 2s)

Table 2 E11 (GPa)	E22 (GPa)	G12 (GPa)	v12	σ11T (MPa)	σ11c (MPa)	τ12 (MPa)
148	7.8	4.5	0.35	2375	1465	95

Table 2 Properties of Isotropic Steel Type

Elastic modulus E(GPa)	Poisson ratio v	mass density ρ (kg / m3)
210	0.3	7800

A tensile load of 119 MPa at one and a lock on the opposite. The fineness of the mesh is optimized in order to have a steady value of maximum stress. To reduce the computation time while maintaining good accuracy, only a quarter of the plate is meshed with progressive mesh designed to produce a very fine mesh around the hole and larger elsewhere (Figure 16).

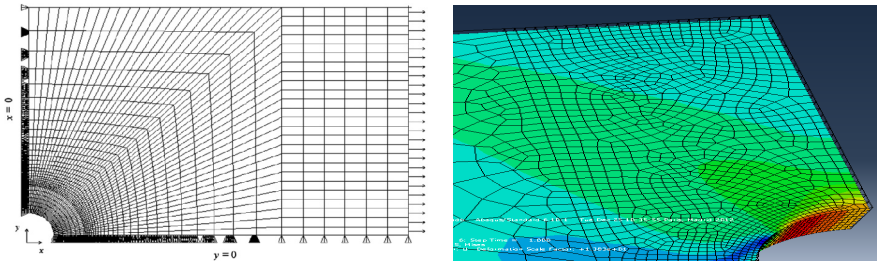

Fig. 16 gradual meshing of the plate

8.2 *Evolution of the Stress Concentration with Diameter Hole (Isotropic Material):*

The results found after an experiment method with camera DIC and with ABAQUS simulation are presented in Table 3:

Table 3 Isotrope Material

a	a/w	Kt infinite	Ktg DIC	Ktg FEA	Ktn DIC	Ktn FEA
0,2	0,02	3	3,0048	3,004	2,82	2,78
2	0,1	3	3,0582	3,04	2,61	2,53
4	0,2	3	3,1900	3,15	2,34	2,21
6	0,3	3	3,4097	3,3	2,22	2,07
8	0,4	3	3,7543	3,6	2,12	1,91
10	0,5	3	4,2937	4,1	2,06	1,81

For a given width, this ratio Kt equal to 3 for an infinitely thin plate with a circular hole and thereafter the global stress concentration factor Ktg increases if the hole diameter increases against the net stress concentration factor Ktn decreases.(Figure 17 and 18):

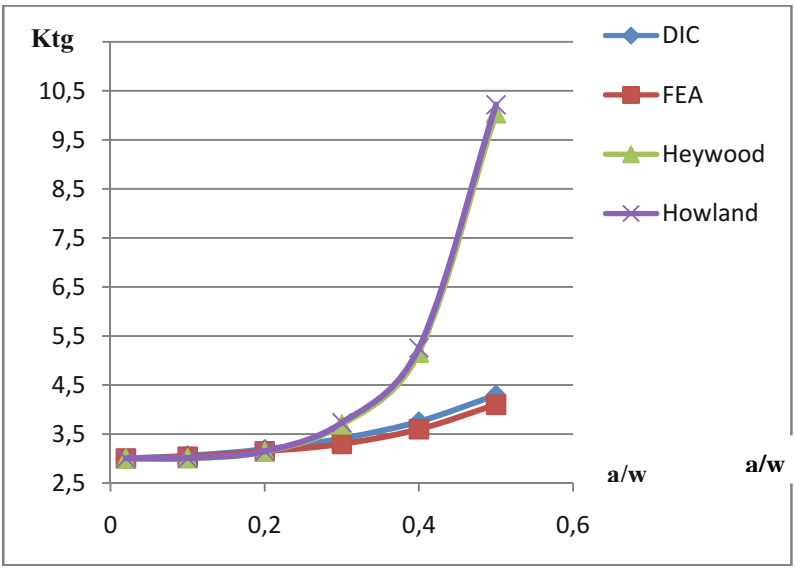

Fig. 17 Variation Ktg isotropic with ratio a/w

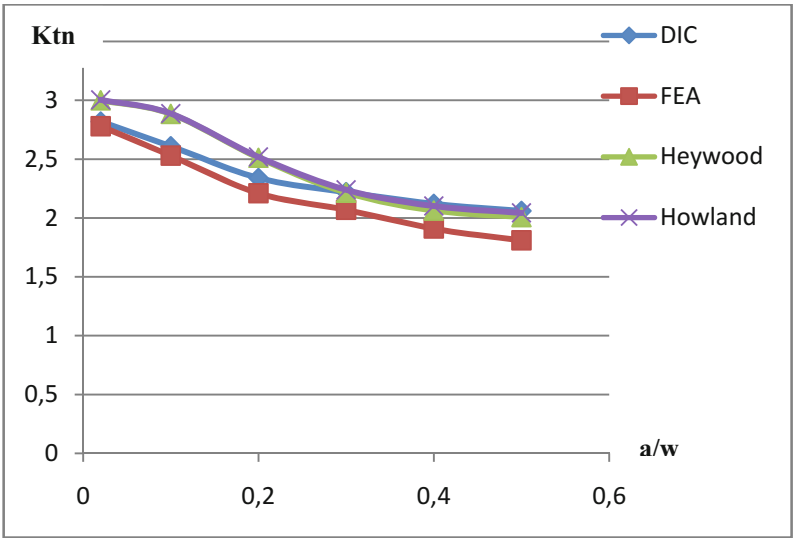

Fig. 18 Variation Ktn isotropic with ratio a/w

For isotropic material we can notes that the results of finite element analysis are very close to the results of DIC camera but for the stress concentration Ktg there is a difference from a / w = 0.4 compared with Heywood and Howland.

8.3 Evolution of the Stress Concentration with Diameter Hole (Orthotropic Material):

Table 4 compares the stress concentration between the finite element analysis and image correlation method:

Table 4 Orthotropic Material

a	a/w	Kt infinite	Ktg (DIC)	Ktg (FEM)	Ktn (DIC)	Ktn (FEM)
0,2	0,01	5,24	3,4	5,41	2,9	4,81
2	0,1	5,24	3,9	6,02	2,72	4,12
4	0,2	5,24	4,52	6,32	2,47	3,2
6	0,3	5,24	5,26	6,62	2,21	2,8
8	0,4	5,24	6,43	7,02	1,82	2,1
10	0,5	5,24	7,12	7,22	1,62	1,7

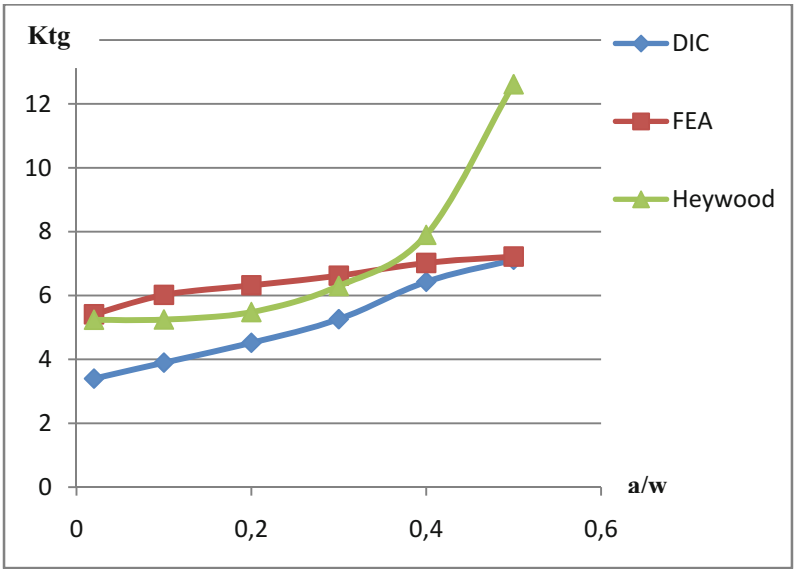

Fig. 19 Variation Ktg orthotropic with ratio a/w

On observed that a / w is increased when the edges of the plate is closer to the hole. Consequently, the lines of force will be more compressed and Ktg increases.

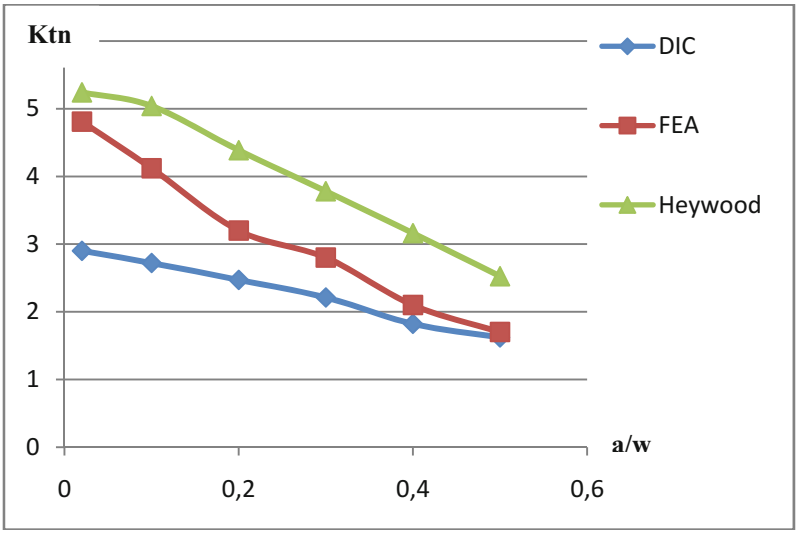

Fig. 20 Variation Ktn orthotropic with ratio a/w

Note that the net stress concentration decreases if the ratio a / w increases and unlike different with global stress concentration factor Ktg.

It has almost the same variation of KTn respect to a/ w for isotropic and orthotropic material.

9 Conclusion

In this work we have used the image correlation method with DIC camera to measure the tensile stress concentration and which gives consistent results with the finite element analysis and thereafter it is found that the DIC method given a best results for a planar structure isotropic or orthotropic.

The results obtained show that the presence of a geometrical discontinuity in a flat plate has a significant effect on the stress concentration to an isotropic and orthotropic material. In addition we see the evolution of global and net stress concentration respect to different hole diameters for composite and steel.

Finally, the DIC approach don't provide good results for composite structures because this method can be show only the surface damage against the composite material having many damage inside the structure (delamination ,cracking matrix….).

Acknowledgements. I want to thank deeply Mr. Jury members who have done me the honor to judge my work and have improved my presentation with helpful comments.

References

[1] Heywood, R.B.: Designing by photoelasticity. Chapman and Hall (1952)
[2] Peterson, R.E.: Stress concentration factors. John Wiley & Sons (1974)
[3] Pilkey, W.D.: Peterson's stress concentration factors, 2nd edn. John Wiley & Sons Inc., New York (1997)
[4] Howland, R.C.J.: On the stresses in the neighborhood of circular hole in a strip under tension. Phil. Trans. Roj. Soc. 229, 49–86 (1929)
[5] Lekhnitskii, S.G.: Theory of Elasticity of an Anisotropic Elastic Body, 1st edn., p. 4. Holden-Day, San Francisco (1963)
[6] Tan, S.C.: Finite-width correction factors for anisotropic plate containing a central opening. J. of Composite Materials 22, 1080–1097 (1988)
[7] Mguil-Touchal, S.: Une technique de corrélation directe d'images numériques. Thèse INSA Lyon (1996)
[8] ASTM D3039/D3039M-00. Standard test method for tensile properties of polymer matrix composite materi-als. American Society for Testing Materials [CD-ROM] (2004)
[9] Howland, R.: On the stresses in the neighborhood of a circular hole in a strip under tension. Philosophical Transactions of the Royal Society A 229, 67 (1929-1930)